

# A Novel Mouse Model for Neurotrophic Keratopathy: Trigeminal Nerve Stereotactic Electrolysis through the Brain

Giulio Ferrari,<sup>1,2,3</sup> Sunil K. Chauhan,<sup>1,2</sup> Hiroki Ueno,<sup>1</sup> Nambi Nallasamy,<sup>1</sup> Stefano Gandolfi,<sup>4</sup> Lawrence Borges,<sup>5</sup> and Reza Dana<sup>1,2</sup>

**PURPOSE.** To develop a mouse model of neurotrophic keratopathy by approaching the trigeminal nerve through the brain and to evaluate changes in corneal cell apoptosis and proliferation.

**METHODS.** Six- to 8-week-old male C57BL/6 mice underwent trigeminal stereotactic electrolysis (TSE) to destroy the ophthalmic branch of the trigeminal nerve. Clinical follow-up using biomicroscopy of the cornea was performed at days 2, 4, 5, and 7. To confirm the effectiveness of the procedure, we examined the gross nerve pathology, blink reflex, and immunohistochemistry of the corneal nerves. TUNEL-positive apoptotic and Ki-67-positive proliferating corneal cells were evaluated to detect changes from the contralateral normal eye.

**RESULTS.** TSE was confirmed by gross histology of the trigeminal nerve and was considered effective if the corneal blink reflex was completely abolished. TSE totally abolished the blink reflex in 70% of mice and significantly reduced it in the remaining 30%. Animals with absent blink reflex were used for subsequent experiments. In these mice, a progressive corneal degeneration developed, with thinning of the corneal epithelium and eventually perforation after 7 days. In all mice, 48 hours after TSE, corneal nerves were not recognizable histologically. Seven days after TSE, an increase in cellular apoptosis in all the corneal layers and a reduction in proliferation in basal epithelial cells were detected consistently in all mice.

**CONCLUSIONS.** TSE was able, in most cases, to induce a disease state that reflected clinical neurotrophic keratitis without damaging the periocular structures. Moreover, corneal denervation led to increased apoptosis and reduced proliferation of epithelial cells, formally implicating intact nerve function in regulating epithelial survival and turnover. (*Invest Ophthalmol Vis Sci.* 2011;52:2532–2539) DOI:10.1167/jovs.10-5688

From the <sup>1</sup>Schepens Eye Research Institute, the <sup>2</sup>Department of Ophthalmology, Massachusetts Eye and Ear Infirmary, and the <sup>3</sup>Neurosurgical Spine Center, Massachusetts General Hospital, Harvard Medical School, Boston, Massachusetts; the <sup>3</sup>G.B. Bietti Eye Foundation, IRCCS, Rome Italy; and the <sup>4</sup>Department of Ophthalmology, University Hospital of Parma, Italy.

Supported in part by National Institutes of Health/National Eye Institute Grant K24 EY019098, Department of Defense Grant W81XWH-09-2-0091 (Schepens Eye Research Institute), and the Bietti Eye Foundation, Rome, Italy.

Submitted for publication April 12, 2010; revised July 28 and October 11, 2010; accepted October 12, 2010.

Disclosure: G. Ferrari, None; S.K. Chauhan, None; H. Ueno, None; N. Nallasamy, None; S. Gandolfi, None; L. Borges, None; R. Dana, None

Corresponding author: Reza Dana, Schepens Eye Research Institute, 20 Staniford Street, Boston, MA 02114; reza.dana@schepens.harvard.edu.

The cornea is the most innervated tissue in the entire human body (400 times more than skin).<sup>1</sup> It receives dense sensory innervation from the trigeminal ganglion and, in some species, modest autonomic innervation. The trigeminal nerve divides into three main branches, one of which, the ophthalmic branch, provides corneal innervation. The organization of corneal nerves, from the depth to the surface of the cornea, is made up of penetrating stromal nerve bundles, subepithelial plexus, sub-basal nerve plexus, and intraepithelial nerve terminals.<sup>2</sup> More than a dozen different neurotransmitters and neuropeptides, whose functions are still incompletely understood, are secreted by corneal nerves.<sup>3</sup>

Corneal nerves are lost because of many pathologic conditions, such as ocular infection, topical anesthetic abuse, surgery, diabetes, stroke, and dry eye syndrome,<sup>1,4–6</sup> which affect millions of people annually. When corneal nerves are severely reduced, neurotrophic keratopathy (NK), a poorly treatable disease, develops. This includes the development of persistent epithelial defects and potentially stromal ulceration that may progress to perforation. However, the exact mechanisms and interactions between trigeminal nerves and corneal cells, including stem cells, epithelial cells, and keratocytes, remain unclear. It is known that nerve-secreted peptides influence corneal cell proliferation in vitro,<sup>7</sup> and corneal epithelial cell mitosis has been shown to be altered in denervated rats.<sup>8,9</sup>

Apoptosis and cell proliferation play key roles in ocular wound healing.<sup>10</sup> Reduced cell proliferation and thinning have been described in the denervated skin<sup>11</sup>; however, it is not known whether enhanced apoptosis or simply reduced cell proliferation is associated with NK. In addition, apoptosis and proliferation have not been studied simultaneously in this condition. This has significant clinical implications because it is a well-known fact that NK patients have delayed healing and often experience persistent epithelial defects<sup>12</sup> and that even minor injuries can seriously threaten ocular integrity.

To address these shortcomings in our current understanding of these important pathophysiologic mechanisms, we have developed, for the first time, a mouse model by removing corneal nerves reproducibly using electrolysis of the ophthalmic branch of the trigeminal nerve with a stereotactic approach, trigeminal stereotactic electrolysis (TSE). This procedure aims to destroy only the fibers providing corneal innervation, leaving the rest of the trigeminal undamaged. Other denervation models have been proposed in monkeys,<sup>13</sup> rabbits,<sup>14–16</sup> and rats.<sup>17,18</sup> NK induction with a hot metal probe through the roof of the mouth has been described in mice; however, no report of death or success rate has been provided, and no stereotactic technique was used.<sup>19</sup> When the same procedure was performed on rats, the authors reported a success rate of 60%, and animals could be kept alive for only 3 to 6 days, which precludes long-term follow-up.<sup>9</sup> Our method represents an advancement of one of the most effective dener-

vation procedures.<sup>20</sup> In addition, this technique applies to the mouse, which is the most widespread experimental mammal used, and is available with the full array of research tools. The procedure was followed by the development of **progressive degeneration** of the corneal tissue, confirmed clinically by biomicroscopy, functionally by examination of the blink reflex, and histologically by the loss of corneal nerves and the degeneration of corneal tissues. Finally, we show histologic evidence of a simultaneous increase in **corneal cell apoptosis** and a reduction in basal epithelial cell proliferation.

## METHODS

### Animals

Five 6- to 8-week-old male C57BL/6 mice (Taconic Farms, Germantown, NY) were used in these experiments. The protocol was approved by the Schepens Eye Research Institute Animal Care and Use Committee, and all animals were treated according to the ARVO Statement for the Use of Animals in Ophthalmic and Vision Research.

### Experimental Procedure

Animals were anesthetized with a ketamine (100 mg/mL)/xylazine (20 mg/mL)/acepromazine (15 mg/mL) mixture. The head of each animal was shaved and disinfected with povidone iodide and ethanol. The animal was then mounted in the stereotactic frame, with particular attention paid to maintaining a sterile field in the surgical area, after which a median incision was made on the skull. The **bregma (the point of conjunction of coronal and sagittal suture)** was identified and chosen as a point of reference. For preliminary anatomic reference, we used a stereotaxic atlas.<sup>21</sup> Experiments on mouse cadavers were performed to calculate the exact stereotactic coordinates. The skull was opened with a dental drill, a **conductive unimodal electrode (FHC, Bowdoin, ME)** was lowered (depth, 0.63 cm) at three different locations (relative to bregma, 0.15 cm anterior and 0.08 cm lateral; 0.09 anterior and 0.10 lateral; 0.09 anterior and 0.12 lateral) on the ophthalmic trigeminal nerve, and a 2-mA current was passed for 15 seconds.

The electrode was removed, and the skin was sutured. A lateral tarsorrhaphy was performed to reduce the risk of infection. Finally, antibiotic ointment (bacitracin-neomycin-polymyxin) was applied to the sutural area and the treated eye. Buprenorphine (0.1 mg/kg body weight every 8 to 12 hours for 72 hours) was injected subcutaneously. The animals were then placed on a heated pad to help the recovery. **Corneal sensitivity** using a cotton filament was recorded preoperatively and postoperatively every 12 hours for 7 days comparing the **blinking** of the treated (left) eye with that of the control (right) eye. All animals were euthanized by carbon dioxide overdose followed by cervical dislocation. All the procedures were performed in the Schepens Eye Research Institute Animal Facility in accordance with an approved protocol.

### Sham Procedure

The sham procedure was conducted by repeating the steps of the experimental procedure (i.e., the electrode was lowered in the same three locations) except that current was not passed through the electrode. Antibiotic ointment was applied to the ipsilateral eye at the end of the procedure.

### Slit Lamp Digital Pictures

Digital pictures of the corneas were taken at the slit lamp at 2, 4, 5, and 7 days after the procedure to check for any change in corneal epithelium or transparency. Particular attention was paid to the detection of **epithelial irregularities** or **corneal edema**.

### Gross Pathology and Histology

To confirm the site of the lesion, the ophthalmic branch of the trigeminal nerve was exposed by careful dissection of the cerebral hemispheres and removal of the surrounding tissues, and digital pictures were taken.

The cornea was harvested and fixed in 4% paraformaldehyde, permeabilized in 0.3% Triton X in PBS with 2% bovine serum albumin for 2 hours, stained with anti- $\beta$ 3 tubulin antibody (rabbit anti-beta 3 tubulin polyclonal antibody; Chemicon, Temecula, CA) overnight at 4°C, and then stained with a secondary conjugated antibody for 2

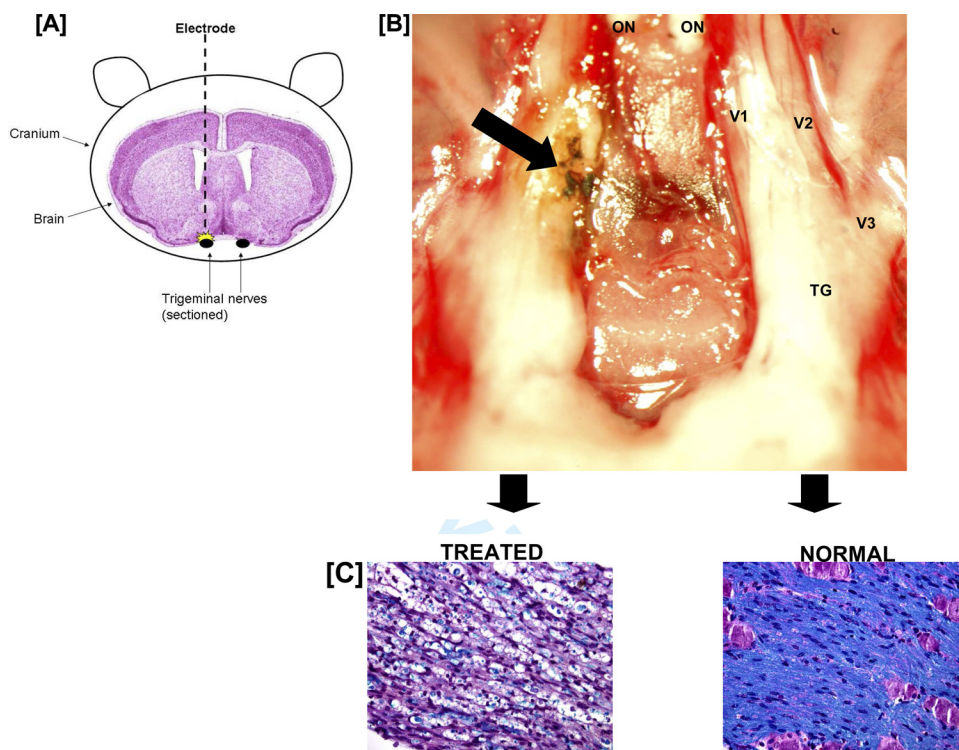


**FIGURE 1.** (A) Scheme of the **TSE** procedure depicted in a coronal section. (B) Gross pathology evidence of trigeminal ablation induced by stereotactic electrolysis. Representative trigeminal nerve lesion induced on left trigeminal nerve (*arrow*). Note the normal contralateral nerve. ON, optic nerve; TG, trigeminal ganglion; V1, V2 (joined), and V3 are, respectively, the ophthalmic, maxillary, and mandibular branches of the trigeminal nerve. (C) TSE induces damage in the trigeminal nerve. Cross-sections taken from the lesioned trigeminal nerve (*left*) and contralateral normal nerve (*right*) stained with Luxol fast blue. Note the extensive disruption and **vacuolization** of the treated tissue. Original magnification, 400 $\times$ . The postmortem examination was performed 7 days after TSE.

hours at room temperature (donkey anti-rabbit IgG FITC; Santa Cruz Biotechnology, Santa Cruz, CA). Both primary and secondary antibodies were diluted to 1:200. Corneal whole mounts were prepared using a DAPI mounting medium (Vectashield mounting medium with DAPI; Vector Laboratories, Burlingame, CA).

### Trigeminal Nerve Histology

Trigeminal nerves were carefully dissected and fixed in 10% formalin overnight. Samples were included in paraffin, and 5- $\mu$ m sections were prepared and stained with Luxol fast blue, as described previously.<sup>22</sup>

### TUNEL Staining

To measure apoptosis we used a specific kit (in situ cell death detection kit, TMR Red; Roche, Nutley, NJ). Eyes were enucleated and prefixed in 4% paraformaldehyde, placed in OCT medium compound (Tissue-Tek; Sakura Finetek, Torrance, CA), and stored at  $-80^{\circ}\text{C}$ . Eight-micrometer cryosections were prepared, postfixed in 4% paraformaldehyde, and stained in accordance with the manufacturer's instructions. Eight corneas were examined (four denervated, four nor-

mal), and four different areas were sampled in each cornea, both in the center and in the periphery. Images were taken at 200 $\times$  magnification.

TUNEL<sup>+</sup>CD45<sup>+</sup> cells were identified by double staining for TUNEL and CD45 marker. Briefly, eyes were enucleated and prefixed in 4% paraformaldehyde, and the cornea was removed and stained for TUNEL as described. Corneas were then stained with CD45 monoclonal conjugated antibody (AlexaFluor 488 anti-mouse CD45 antibody; BioLegend, San Diego, CA) and mounted. Images were taken at 400 $\times$  magnification.

### Ki-67 Staining

For measuring proliferation, enucleated globes were placed in OCT compound, and sagittal sections measuring 8  $\mu$ m were cut with a cryostat and placed on glass slides. Slides were fixed in acetone, rinsed in PBS, and blocked with 1% bovine serum albumin. Sections were then processed for immunohistochemical and morphologic evaluations. Actively proliferating cells were identified by immunofluorescence using a FITC-conjugated mouse monoclonal antibody against the Ki-67 protein (Novocastra Laboratories, Newcastle, UK), a cell proliferation marker expressed during active phases of the cell cycle.<sup>23</sup> The

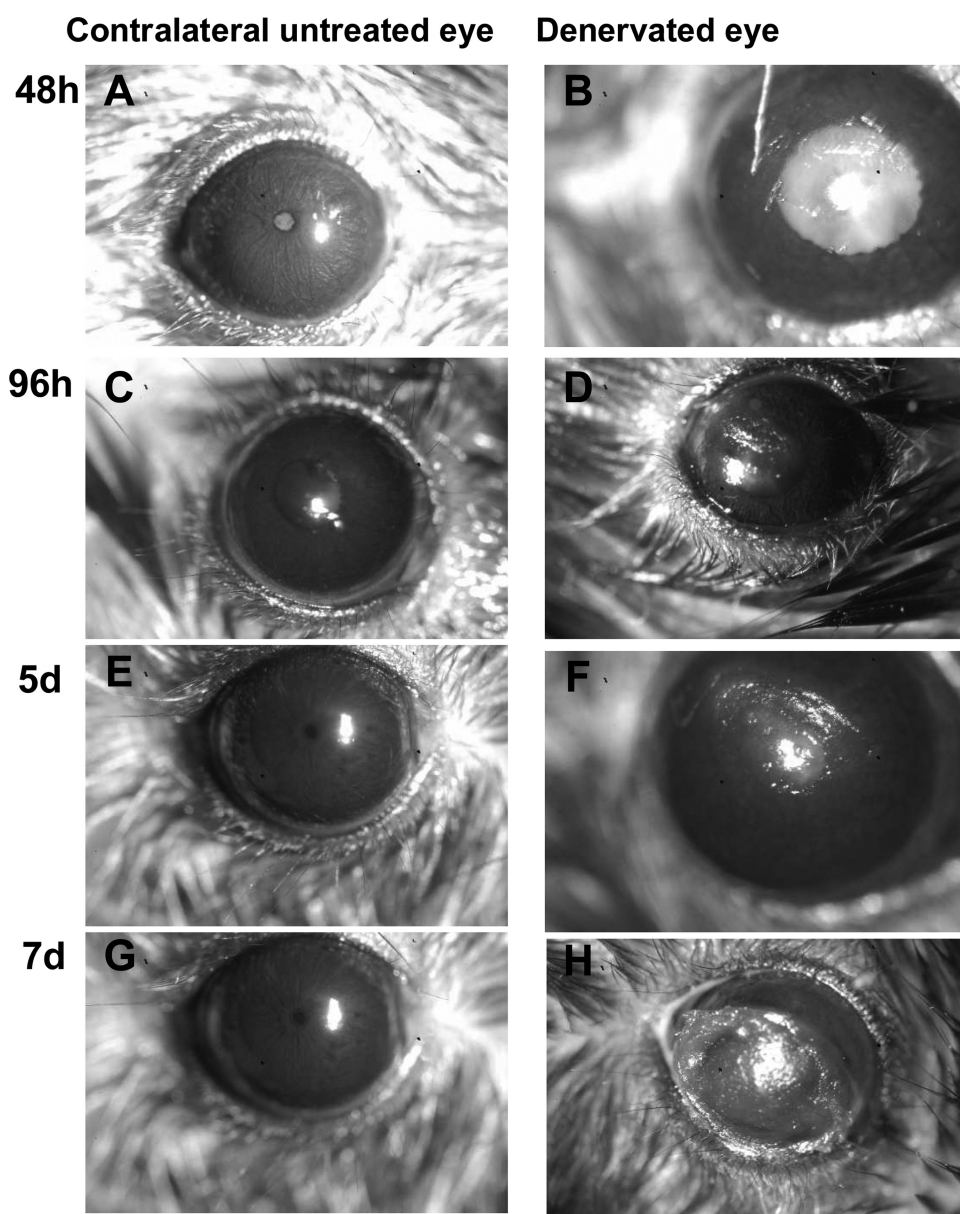


**FIGURE 2.** Representative slit lamp photographs demonstrating the development of neurotrophic keratopathy at different time points after unilateral central trigeminal electrocoagulation compared with the contralateral side. (A, C, E, G) Normal contralateral eye. (B, D, F, H) Denervated eye. Functional testing of blink reflex was performed by touching the cornea with a cotton thread. Note the absence of blink reflex (arrow). (B). Starting 48 hours after the procedure, the development of punctate keratopathy was observed (B). This extended progressively (D, F) to form a confluent area of severe epithelial defect (H). The contralateral cornea retained transparency (A, C, E, G) and a normal blink reflex.



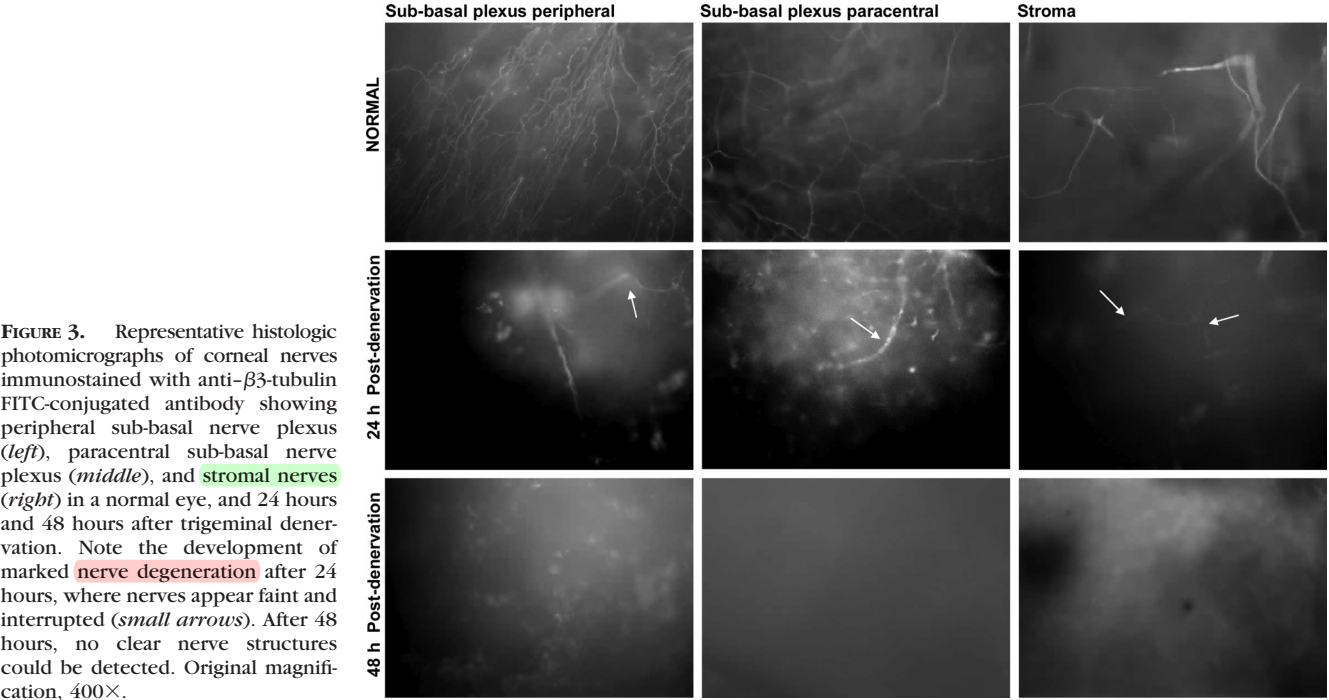


**FIGURE 3.** Representative histologic photomicrographs of corneal nerves immunostained with anti- $\beta$ 3-tubulin FITC-conjugated antibody showing peripheral sub-basal nerve plexus (left), paracentral sub-basal nerve plexus (middle), and stromal nerves (right) in a normal eye, and 24 hours and 48 hours after trigeminal denervation. Note the development of marked nerve degeneration after 24 hours, where nerves appear faint and interrupted (small arrows). After 48 hours, no clear nerve structures could be detected. Original magnification, 400 $\times$ .

antibody was diluted 1:100 and placed on the sections, and cryosections were prepared. We examined eight corneas (four denervated and four normal) and sampled four areas in each cornea centrally. All digital pictures were taken under a fluorescence microscope (E800; Nikon, Melville, NY) with a 600 $\times$  magnification.

Epithelial Thickness

To study the effect of the procedure on epithelial thickness, whole globes were removed and fixed in OCT cryoprotectant medium and stored in  $-80^{\circ}\text{C}$ . Eight-micrometer cryosections were cut. We exam-

ined 10 eyes (five denervated and five normal) in four different areas in the central cornea. Corneal epithelial thickness was determined using automated image analysis software (MatLab; The MathWorks Inc., Natick, MA). Epithelium was segmented from microscopic corneal images using morphologic techniques. Thickness measurements were determined by averaging more than three sampled locations per image.

Blink Reflex Evaluation

The blink reflex was tested with a cotton thread, both in the central and the peripheral cornea, immediately after animal recovery from

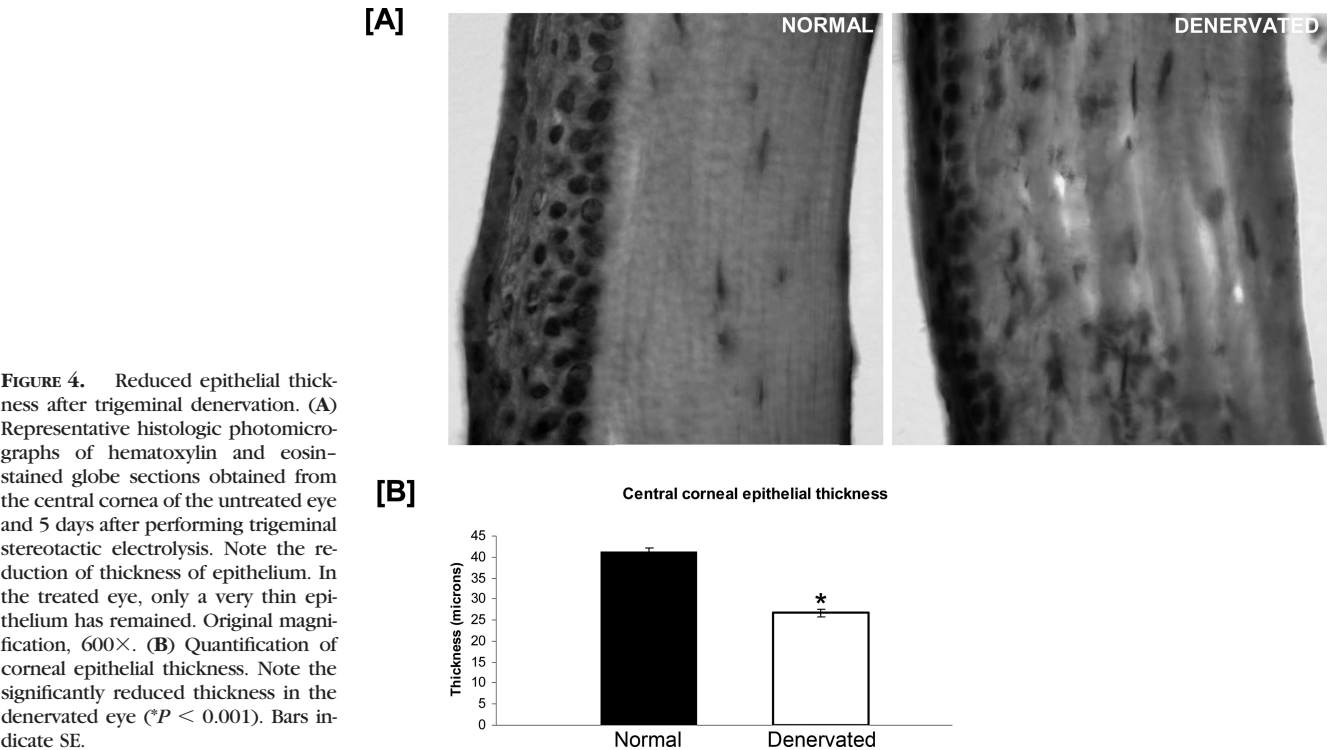


**FIGURE 4.** Reduced epithelial thickness after trigeminal denervation. (A) Representative histologic photomicrographs of hematoxylin and eosin-stained globe sections obtained from the central cornea of the untreated eye and 5 days after performing trigeminal stereotactic electrolysis. Note the reduction of thickness of epithelium. In the treated eye, only a very thin epithelium has remained. Original magnification, 600 $\times$ . (B) Quantification of corneal epithelial thickness. Note the significantly reduced thickness in the denervated eye (\* $P < 0.001$ ). Bars indicate SE.

anesthesia and then every 12 hours until the animals were euthanized. Unanesthetized mice were tested for the blink reflex by touching the center and the periphery of the cornea with a sterile filament of cotton, under a dissecting microscope (magnification 10 $\times$ ), to avoid touching the whiskers and eyelashes, as previously described.<sup>24</sup> Only animals showing absence of reflex at all times were used for the experiments.

## RESULTS

### Electrocoagulation of the Ophthalmic Branch of the Trigeminal Nerve

A schematic diagram showing a coronal view of the TSE procedure is provided in Figure 1A. After TSE, gross pathology of the trigeminal nerve revealed a lesion in the left ophthalmic branch (Fig. 1B). A characteristic burn induced by the electrocoagulation could be seen at the site of the electrode penetration (the ophthalmic branch). On histochemical analysis, the treated trigeminal nerve tissue showed extensive disruption and vacuolization compared with the untreated, contralateral nerve (Fig. 1C).

The maxillary and mandibular branches appeared intact. This was further confirmed as recovered animals responded to the touch of the respective innervated areas. The optic nerves were intact. No apparent hemorrhage or lesion was evident in the ganglion, hemispheres, or outside the targeted area. The sham procedure was not associated with any changes.

### In Vivo Evaluation of Corneal Integrity and Blinking Reflex

Biomicroscopy of the cornea showed a progressive development of keratopathy; this started as punctate keratopathy 48 hours after the procedure, which progressively coalesced to diffuse epitheliopathy 7 days later (Fig. 2). When the sham procedure was performed (i.e., electrode was lowered but no current passed), the cornea remained normal and the blink reflex was maintained at all time points. The epithelium imaged at the slit lamp showed areas of disruption 24 hours after the procedure, which increased after 48 hours (Fig. 2). The blink reflex, tested with a cotton thread, was found to be totally absent in 70% of animals treated and significantly reduced in the remaining 30% (Fig. 2B). Only animals with totally absent reflex both in the central and the peripheral cornea at all time points were used in this study.

### Ex Vivo Evaluation of Corneal Innervation

In nontreated contralateral eyes, the subbasal nerve plexus and thick stromal trunks were normally present. In the TSE group, 24 hours after denervation, the subbasal nerve plexus lost its characteristic branching pattern. Moreover, the stromal nerves in the TSE group appeared faint and disrupted at various points. At 48 hours, no clear nerve structure could be detected either in the subbasal nerve plexus or the stroma (Fig. 3).

### Thickness of Corneal Epithelial Cell Layer

Globe cross-sections stained with hematoxylin-eosin 5 days after the procedure were prepared and showed a reduction in

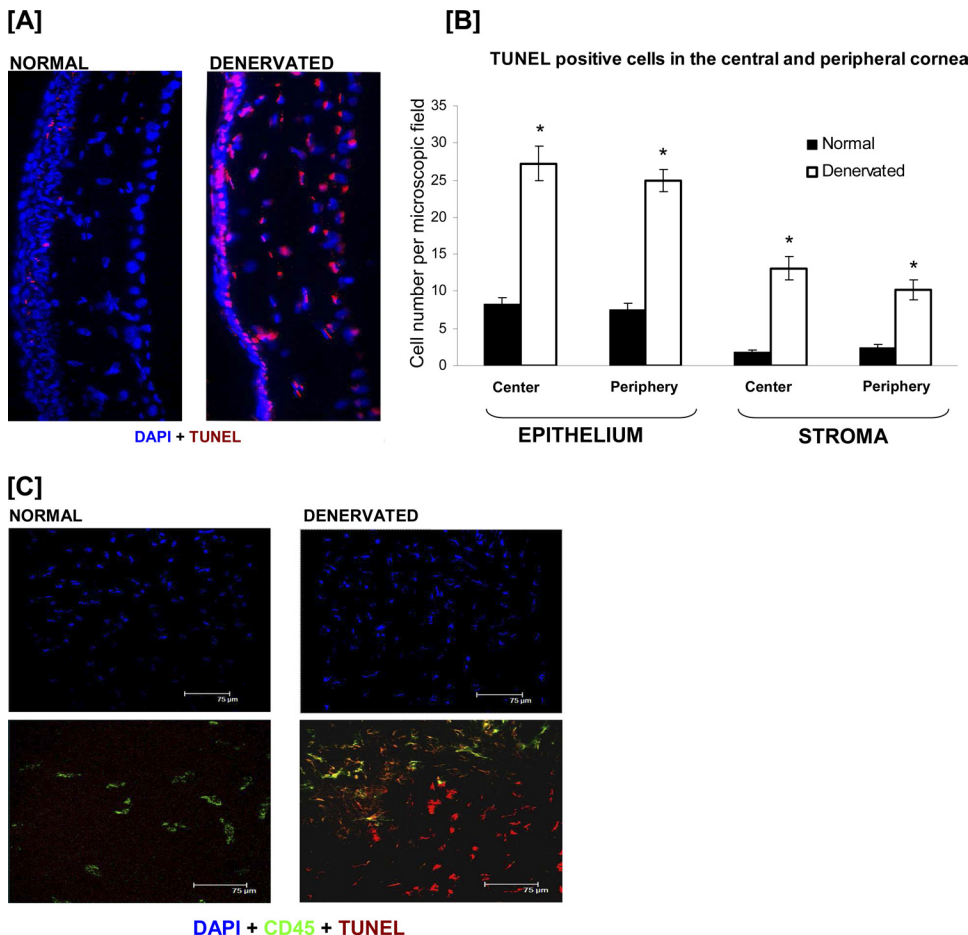


**FIGURE 5.** Increased corneal apoptosis after trigeminal denervation. (A) Apoptosis in normal and denervated corneal cross-sections detected by TUNEL technique. Nuclei are stained with DAPI. Normal cornea: note the multilayered epithelium and the scarce number of apoptotic cells, which are mainly located in the superficial epithelium. Denervated cornea: note the extremely thin epithelium, which is reduced to a few layers, and the numerous apoptotic cells, which are located throughout the cornea. (B) Quantification of apoptotic cells in the epithelium and stroma of the central and peripheral cornea. Note the significantly increased apoptosis in the denervated cornea (\* $P < 0.001$ ). Number of TUNEL<sup>+</sup> cells per microscopic field was counted at 200 $\times$  magnification. Bars indicate SE. (C) Representative micrographs of corneal whole mounts showing phenotypes of apoptotic cells in the stroma. Increased keratocyte and inflammatory cell (CD45<sup>+</sup>) apoptosis after denervation. Note the infiltration of CD45<sup>+</sup> cells after TSE and the presence of TUNEL<sup>+</sup>CD45<sup>+</sup> cells suggesting that keratocytes are also undergoing apoptosis. Original magnification, 400 $\times$ .

the epithelial thickness (mean, 35%) (Fig. 4A). The epithelial thickness was significantly reduced ( $P < 0.001$ ) in the denervated eye compared with the normal contralateral eye (Fig. 4B). In addition, we found infiltration of inflammatory cells that was located primarily in the anterior stroma, in the denervated corneas.

### Apoptosis of Corneal Cells

Immunohistochemistry for TUNEL<sup>+</sup> apoptotic cells was performed 7 days after denervation. TUNEL<sup>+</sup> cells in the epithelium, stroma, and endothelium of the denervated eye were identified under the microscope and counted. Two areas were considered: central and peripheral (limbal) cornea. In the normal eye, few epithelial cells were TUNEL<sup>+</sup>, and they were located primarily in the outer superficial layers (Fig. 5A). In the diseased eye, an increased number of TUNEL<sup>+</sup> cells were detected diffusely scattered in the epithelium, stroma, and even the endothelium. More specifically, we observed a 70% increase in apoptotic cells in both the central and the peripheral epithelium and 86% and 76% increases in the central and peripheral stroma, respectively, compared with normal eyes (Fig. 5B). The difference in the TUNEL<sup>+</sup> cell counts between normal and denervated eyes was statistically significant ( $P < 0.001$ ). Further, to characterize the phenotype of these cells, we performed corneal whole mount staining for CD45 and TUNEL. On comparison between denervated and nondenervated corneal stromas, we noticed significant increases in the numbers of both live (TUNEL<sup>-</sup>) and dead (TUNEL<sup>+</sup>) CD45<sup>+</sup> cells in denervated eyes. In addition, we found an increase in the CD45<sup>+</sup> TUNEL<sup>+</sup> cells in denervated eyes, suggesting increased apoptosis of keratocytes (Fig. 5C).

### Proliferation of Basal Epithelial Cells

Immunohistochemistry for Ki-67 performed on globe cross-sections 7 days after denervation showed a reduction of Ki-67<sup>+</sup> cells in the basal epithelial layer of the denervated eyes, though they were normally present in the normal contralateral eyes (Fig. 6A). When we compared the number of Ki-67<sup>+</sup> cells in normal and denervated eyes, we found a reduction of 90% in the latter ( $P < 0.001$ ) (Fig. 6B).

## DISCUSSION

The prevalence of NK is unknown, but it is probably underestimated given that reduction in corneal sensation is a common clinical observation in most severe chronic corneal diseases. In spite of significant efforts to unravel the pathophysiology of NK, it is not yet clear why NK patients have delayed healing times because they often present with persistent epithelial defects, and even minor injuries can seriously threaten ocular integrity.<sup>12</sup> Reduced mitosis of the epithelial cells has been demonstrated,<sup>8,9</sup> but no report about the role of apoptosis in NK has been produced, nor has its coexistence with proliferation reduction been evaluated. To test whether denervation influences cell proliferation or apoptosis, we developed the TSE, a procedure aimed at inducing NK in mice without surgical or experimental manipulation of the globe or periocular tissues. In addition, to better understand NK pathophysiology, a reproducible murine model would be helpful to test new therapies. We also propose this method could be used to study the effect of trigeminal denervation in ocular tissues different from the cornea (such as the anterior chamber, retina, and choroid) because little is known about the physiologic relevance of trigeminal innervation to the eye.

In this study, we demonstrated a reproducible surgical approach, TSE, that induces corneal nerve disruption and is followed by the development of an epithelial and stromal

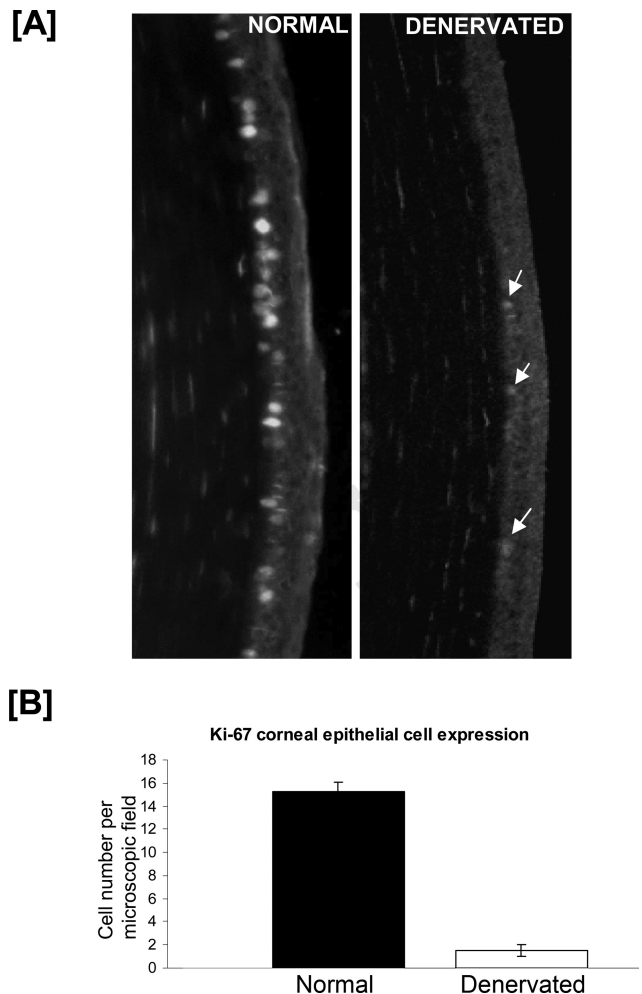


**FIGURE 6.** Reduced basal epithelial cell proliferation after trigeminal denervation. (A) Ki-67 detection of proliferating basal epithelial cell in cornea cross-sections. Note the numerous Ki-67<sup>+</sup> cells in the normal corneal basal epithelium. After trigeminal denervation, the number of Ki-67<sup>+</sup> cells is significantly reduced, and only a few faintly stained basal cells can be detected (arrows). (B) Quantification of Ki-67<sup>+</sup> cells in normal and denervated corneas. Note the reduction in proliferating cells after denervation ( $*P < 0.001$ ). Number of Ki-67<sup>+</sup> cells per microscopic field was counted at 600 $\times$  magnification. Bars indicate SE.

disease highly resemblant of human NK. We demonstrated the site of the lesion in the trigeminal nerve and its peripheral effect on corneal nerve degeneration. Our approach requires 30 minutes and leaves the eye and orbital structures untouched, and it does not require the application of any chemical substance to the eye or periocular structures that could potentially introduce confounding factors. Attempts to remove corneal nerves with toxins (such as capsaicin<sup>25,26</sup> or other neurotoxins<sup>27,28</sup>) or to surgically denervate by axotomy in the orbital cavity can cause significant perturbation of the microenvironment and could induce inflammation or cell apoptosis as a result of trauma itself. For example, capsaicin injection specifically affects all sensory neurons in the body, and it has been shown to change the level of brain derived neurotrophic factor in the dorsal root ganglions.

Several neurotrophic keratopathy models have been described in rats,<sup>17,18,20</sup> rabbits,<sup>14–16</sup> and monkeys.<sup>13</sup> However, to our knowledge, a reproducible mouse model that could circumvent these issues (e.g., of inducing significant anatomic disruption around the eye or inducing chemical injury to the ocular surface, as with ethanol) approaching the trigeminal



nerve from the brain has not yet been described. We believe this can represent a significant improvement, given the low cost and the wide array of murine reagents for the study of pathophysiologic mechanisms and the wide availability of transgenic and knockout models.

Tissue homeostasis in normal physiology is controlled by a tight regulation of apoptosis and proliferation, and it is interesting to speculate that the balance between these two mechanisms is perturbed in neurotrophic keratopathy. Apoptosis, also known as programmed cell death, plays a major role in most mechanisms of regulation of differentiation and wound healing.<sup>10</sup> Denervation has a dramatic effect on the apoptosis of myocytes<sup>29</sup> and Leydig cells.<sup>30</sup> In the cornea, apoptosis has been shown to occur after infection,<sup>31</sup> surgery,<sup>32</sup> or topical drug application.<sup>33</sup> However, no report has described the impact of denervation on corneal apoptosis. Apoptosis has been related to corneal opacity<sup>34</sup> and punctate keratopathy,<sup>35</sup> which we found in the TSE-treated eyes. In our study, we found apoptosis increased after TSE. Interestingly, although in normal eyes apoptosis was found at a background level primarily in the superficial epithelium, consistent with normal tissue turnover, we noted that 7 days after denervation, apoptosis was also extensively detected in keratocytes and even endothelial cells, suggesting a trophism support of nerves beyond just the epithelium. Interestingly, apoptotic cells were found diffusely scattered in all corneal layers, whereas the majority of inflammatory cells were located in the anterior stroma, hence suggesting that resident corneal cells were undergoing apoptosis. To better assess the phenotype of corneal cells undergoing apoptosis, we performed double staining for TUNEL and CD45 (as a marker of inflammatory cells) and found that TUNEL<sup>+</sup>CD45<sup>+</sup> cells, which could presumably be considered resident keratocytes, were increased after denervation.

Various neuropeptides found in the cornea, such as substance P (SP),<sup>36</sup> calcitonin gene-related peptide (CGRP),<sup>37</sup> and nerve growth factor (NGF),<sup>38</sup> have antiapoptotic properties, and their reduction or disappearance after denervation could explain our findings. Corneal nerve-secreted peptides such as SP,<sup>39</sup> NGF,<sup>40,41</sup> and glial-derived neurotrophic factor,<sup>41</sup> have also been shown to support the proliferation of corneal cells. It has also been shown that corneal denervation induces a reduction of epithelial cell mitosis in rats,<sup>8,9</sup> but no information is available in mice.

We evaluated actively proliferating corneal cells by staining for Ki-67 protein, a cell proliferation marker expressed during the active phases of the cell cycle (G1, S, G2, and mitosis) but absent from resting cells (G0).<sup>42</sup> Ki-67 has been used to identify proliferating corneal epithelial cells.<sup>43</sup> We found Ki-67 expression reduced after TSE. We also detected reduced epithelial thicknesses in the central cornea.<sup>43,44</sup> Interestingly, this is similar to what has been reported for the denervated epidermis in which keratinocyte proliferation was also reduced.<sup>11</sup> The epidermis shares anatomic similarity with the cornea because it is also surface ectoderm-derived; however, it is a keratinized epithelium. Our findings support the general theory of a specific neurotrophic effect on ectodermal tissues, which has been proposed by various authors.<sup>46,47</sup>

The penetration of the electrode through the brain to reach the trigeminal nerve can be complicated by meningoencephalitis<sup>23</sup>; however, we did not notice neurologic or autaptic signs of development of brain infections in our animals. This could be partly due to the fact that we followed a rigorous aseptic technique. We do not know to what extent other factors (i.e., inflammation) participated in the development of NK; however, this will be the subject of further studies. In addition, the trajectory of the electrode through the brain tissue could theoretically alter the release of neuropeptides in the cornea. However, when we performed a sham procedure (i.e., same

procedure with lowering of the electrode to the trigeminal nerve without passing current), the ipsilateral eye remained normal. TSE was effective in totally abolishing the blink reflex in 70% of cases, and the animal survival rate free of neurologic complications such as paralysis was 90%. Because it has been shown that in some cases the cornea receives innervation from the maxillary branch of the trigeminal nerve,<sup>18,47,48</sup> we hypothesize that our specific lesion of the ophthalmic branch may spare these fibers in some animals, thereby allowing retention of some sensation in a minority of cases.

The development and clinical evolution of NK after TSE was rapid (7 days) compared to what has been shown in rats<sup>17,18,20</sup> and what is observed in humans, possibly because of various reasons. First, mice are smaller than rats, and it is possible that the time required for nerve degeneration is shorter given the shorter fibers. Second, we included in our study only animals with complete corneal anesthesia, defined by the complete absence of corneal reflex, which presumably would experience the most severe form of NK. Third, human patients often undergo some sort of therapy, which slows down the course of the disease, and reduced sensation is more common than complete corneal anesthesia.

In conclusion, our findings support the importance of corneal nerves on the two main mechanisms of tissue homeostasis: apoptosis and cell proliferation. We emphasize that the adoption of our animal model could provide a useful tool in dissecting the role of nerves on various adult and stem cell populations in the cornea and, more widely, could be a paradigm of nerve-tissue interactions in health and disease, ultimately facilitating the development of new therapies.

## Acknowledgments

The authors thank Jessica Lanzim for help with the animal care and Don Pottle and Qiang Zhang for the excellent technical assistance.

## References

- Rozsa AJ, Beuerman RW. Density and organization of free nerve endings in the corneal epithelium of the rabbit. *Pain*. 1982;14:105-120.
- Al-Aqaba M, Fares U, Suleman H, Lowe J, Dua HS. Architecture and distribution of human corneal nerves. *Br J Ophthalmol*. 2010;94:784-789.
- Muller LJ, Marfurt CF, Kruse F, Tervo TM. Corneal nerves: structure, contents and function. *Exp Eye Res*. 2003;76:521-542.
- Epstein DL, Paton D. Keratitis from misuse of corneal anesthetics. *N Engl J Med*. 1968;279:396-399.
- Benitez del Castillo JM, Wasfy MA, Fernandez C, Garcia-Sanchez J. An in vivo confocal masked study on corneal epithelium and subbasal nerves in patients with dry eye. *Invest Ophthalmol Vis Sci*. 2004;45:3030-3035.
- Kaufman SC. Anterior segment complications of herpes zoster ophthalmicus. *Ophthalmology*. 2008;115:S24-S32.
- Garcia-Hirschfeld J, Lopez-Briones LG, Belmonte C. Neurotrophic influences on corneal epithelial cells. *Exp Eye Res*. 1994;59:597-605.
- Sigelman S, Dohlman CH, Friedenwald JS. Mitotic and wound healing activities in the rat corneal epithelium: influence of various hormones and endocrine glands. *Arch Ophthalmol*. 1954;52:751-757.
- Sigelman S, Friedenwald JS. Mitotic and wound-healing activities of the corneal epithelium: effect of sensory denervation. *Arch Ophthalmol*. 1954;52:46-57.
- Salomao MQ, Wilson SE. Corneal molecular and cellular biology update for the refractive surgeon. *J Refract Surg*. 2009;25:459-466.
- Huang IT, Lin WM, Shun CT, Hsieh ST. Influence of cutaneous nerves on keratinocyte proliferation and epidermal thickness in mice. *Neuroscience*. 1999;94:965-973.

12. Jeng BH, Dupps WJ Jr. Autologous Serum 50% eyedrops in the treatment of persistent corneal epithelial defects. *Cornea*. 2009; 28:1104-1108.
13. Oduntan O, Ruskell G. The source of sensory fibres of the inferior conjunctiva of monkeys. *Graefe's Arch Clin Exp Ophthalmol*. 1992;230:258-263.
14. Schimmelpfennig B, Beuerman R. A technique for controlled sensory denervation of the rabbit cornea. *Graefe's Arch Clin Exp Ophthalmol*. 1982;218:287-293.
15. Schimmelpfennig B, Beuerman RW. Sensory denervation of the rabbit cornea affects epithelial properties. *Exp Neurol*. 1980;69: 196-201.
16. Gilbard JP, Rossi SR. Tear film and ocular surface changes in a rabbit model of neurotrophic keratitis. *Ophthalmology*. 1990;97: 308-312.
17. Wong EK, Kinyamu RD, Graff JM, et al. A rat model of radiofrequency ablation of trigeminal innervation via a ventral approach with stereotaxic surgery. *Exp Eye Res*. 2004;79:297-303.
18. Tervo T, Joo F, Huikuri KT, Toth I, Palkama A. Fine structure of sensory nerves in the rat cornea: an experimental nerve degeneration study. *Pain*. 1979;6:57-70.
19. Zander E, Weddell G. Reaction of corneal nerve fibers to injury. *Br J Ophthalmol*. 1951;35:61-88.
20. Nagano T, Nakamura M, Nakata K, et al. Effects of substance P and IGF-1 in corneal epithelial barrier function and wound healing in a rat model of neurotrophic keratopathy. *Invest Ophthalmol Vis Sci*. 2003;44:3810-3815.
21. Paxinos G, Franklin KBJ. *The Mouse Brain in Stereotaxic Coordinates*. 2nd ed. San Diego: Academic Press; 2001.
22. Saadoun S, Tait MJ, Reza A, Davies DC, Bell BA, Verkman AS, Papadopoulos MC. AQP4 gene deletion in mice does not alter blood-brain barrier integrity or brain morphology. *Neuroscience*. 2009;7:161:764-772.
23. Brown DC, Gatter KC. Ki67 protein: the immaculate deception? *Histopathology*. 2002;40:2-11.
24. Tullo AB, Shimeld C, Blyth WA, Hill TJ, Easty DL. Ocular infection with herpes simplex virus in nonimmune and immune mice. *Arch Ophthalmol*. 1983;101:961-964.
25. Keen P, Tullo AB, Blyth WA, Hill TJ. Substance P in the mouse cornea: effects of chemical and surgical denervation. *Neurosci Lett*. 1982;29:231-235.
26. Hiura A, Nakagawa H. Capsaicin-resistant, nonspecific acetylcholinesterase (NsAChE) reactive nerve fibers in the rat cornea: a quantitative and developmental study. *Okajimas Folia Anatomica Japonica*. 2004;81:75-84.
27. Gallar J, Garcia de la Rubia P, Gonzalez GG, Belmonte C. Irritation of the anterior segment of the eye by ultraviolet radiation: influence of nerve blockade and calcium antagonists. *Curr Eye Res*. 1995;14:827-835.
28. Olurin O, Osuntokun O. Complications of retrobulbar alcohol injections. *Ann Ophthalmol*. 1978;10:474-476.
29. Siu PM. Muscle apoptotic response to denervation, disuse, and aging. *Med Sci Sports Exercise*. 2009;41:1876-1886.
30. Gong YG, Wang YQ, Gu M, Feng MM, Zhang W, Ge RS. Deprivation of testicular innervation induces apoptosis of Leydig cells via caspase-8-dependent signaling: a novel survival pathway revealed. *Biochem Biophys Res Commun*. 2009;382:165-170.
31. Zhou Z, Bar rett RP, McClellan SA, et al. Substance P delays apoptosis, enhancing keratitis after *Pseudomonas aeruginosa* infection. *Invest Ophthalmol Vis Sci*. 2008;49:4458-4467.
32. Brignole F, Auzeir O, Baudouin C. Apoptosis and the ocular surface. *J Francais d'Ophtalmol*. 2003;26:299-306.
33. Song JS, Kim JH, Yang M, Sul D, Kim HM. Mitomycin-C concentration in cornea and aqueous humor and apoptosis in the stroma after topical mitomycin-C application: effects of mitomycin-C application time and concentration. *Cornea*. 2007;26:461-467.
34. Van Meter WS. Central corneal opacification resulting from recent chemotherapy in corneal donors. *Trans Am Ophthalmol Soc*. 2007;105:207-212.
35. Kojima T, Higuchi A, Goto E, Matsumoto Y, Dogru M, Tsubota K. Autologous serum eye drops for the treatment of dry eye diseases. *Cornea*. 2008;27(suppl 1):S25-S30.
36. Huang B, Fu H, Yang M, Fang F, Kuang F, Xu F. Neuropeptide substance P attenuates hyperoxia-induced oxidative stress injury in type II alveolar epithelial cells via suppressing the activation of JNK pathway. *Lung*. 2009;187:421-426.
37. Chan JJ, Farmer PJ, Southwell BR, Sourial M, Hutson JM. Calcitonin gene-related peptide is a survival factor, inhibiting apoptosis in neonatal rat gubernaculum in vitro. *J Pediatr Surg*. 2009;44:1497-1501.
38. Kishi S, Shimoke K, Nakatani Y, et al. Nerve growth factor attenuates 2-deoxy-d-glucose-triggered endoplasmic reticulum stress-mediated apoptosis via enhanced expression of GRP78. *Neurosci Res*. 2010;66:14-21.
39. Reid TW, Murphy CJ, Iwahashi CK, Foster BA, Mannis MJ. Stimulation of epithelial cell growth by the neuropeptide substance P. *J Cell Biochem*. 1993;52:476-485.
40. Kruse FE, Tseng SC. Growth factors modulate clonal growth and differentiation of cultured rabbit limbal and corneal epithelium. *Invest Ophthalmol Vis Sci*. 1993;34:1963-1976.
41. You L, Kruse FE, Volcker HE. Neurotrophic factors in the human cornea. *Invest Ophthalmol Vis Sci*. 2000;41:692-702.
42. Scholzen T, Gerdes J. The Ki-67 protein: from the known and the unknown. *J Cell Physiol*. 2000;182:311-322.
43. Fabiani C, Barabino S, Rashid S, Dana MR. Corneal epithelial proliferation and thickness in a mouse model of dry eye. *Exp Eye Res*. 2009;89:166-171.
44. Henriksson JT, McDermott AM, Bergmanson JP. Dimensions and morphology of the cornea in three strains of mice. *Invest Ophthalmol Vis Sci*. 2009;50:3648-3654.
45. Albers KM, Davis BM. The skin as a neurotrophic organ. *Neuroscientist*. 2007;13:371-382.
46. Roosterman D, Goerge T, Schneider SW, Bunnett NW, Steinhoff M. Neuronal control of skin function: the skin as a neuroimmunoenocrine organ. *Physiol Rev*. 2006;86:1309-1379.
47. Ruskell GL. Ocular fibres of the maxillary nerve in monkeys. *J Anat*. 1974;118:195-203.
48. Marfurt CF, Kingsley RE, Echtenkamp SE. Sensory and sympathetic innervation of the mammalian cornea: a retrograde tracing study. *Invest Ophthalmol Vis Sci*. 1989;30:461-472.